Lawrence Berkeley Laboratory
UNIVERSITY OF CALIFORNIA

Submitted to Nuclear Physics

ANGULAR MOMENTUM MISALIGNMENT IN DEEP INELASTIC PROCESSES AND ANGULAR DISTRIBUTION OF SEQUENTIALLY EMITTED PARTICLES AND GAMMA RAYS

L.G. Moretto, S. Blau, and A. Pacheco

December 1980

Prepared for the U.S. Department of Energy under Contract W-7405-ENG-48

DISCLAIMER

ANGULAR MOMENTUM MISALIGNMENT IN DEEP INELASTIC PROCESSES AND ANGULAR DISTRIBUTION OF SEQUENTIALLY EMITTED PARTICLES AND GAMMA RAYS*

L. G. Moretto, S. Blau and A. Pacheco

Department of Chemistry and Nuclear Science Division
Lawrence Berkeley Laboratory
University of California
Berkeley, CA 94720

Abstract

The angular momentum misalignment for fragments produced in deep inelastic scattering is discussed in terms of the thermal excitation of angular-momentum-bearing modes in the intermediate complex. Analytical expressions for the in- and out-of-plane angular distributions are obtained for sequentially emitted particles and fission fragments. The angular momentum dependence of the ratio between particle and neutron decay width is explicitly treated and found to be quite important. Similarly angular distributions are obtained both for dipole and quadrupole gamma decay. The theoretical results are compared with experimental angular distributions of sequential fission fragments, sequential alphas and gamma rays and a good agreement is found.

---

*This work was supported by the Nuclear Science Division of the U. S. Department of Energy under contract No. W-7405-ENG-48.

Introduction

In heavy ion collisions leading to deep inelastic reactions one observes the formation of a partially equilibrated, relatively short-lived intermediate complex, or dinuclear system.[1] During the collision, angular momentum is transferred from orbital motion to intrinsic rotation.[2-5] Furthermore, additional angular momentum can be generated in the two nuclei by the excitation of angular-momentum-bearing modes of the intermediate complex.[6]

Several determinations of the magnitude of the transferred angular momentum have been performed, mostly by measuring the associated gamma ray multiplicities, both as a function of the Q value and of the exit channel mass asymmetry.[2-5] There is, in general, an increase of the transferred angular momentum with increasing Q value.[2] Frequently the secular equilibrium limit of rigid rotation seems to be attained.[4,5] This is especially clear in reactions involving narrow ℓ-windows, where the characteristic rise of the total fragment spin with increasing exit channel asymmetry has been observed.[4,5]

Just as interesting as the magnitude of the transferred angular momentum is its alignment. Angular momentum misalignment occurs when in-plane components of the angular momentum are present. These components can be generated either directly by some unknown feature of the reaction mechanism, or can be associated with thermal fluctuations of the angular-momentum-bearing modes of the intermediate complex. In a theoretical investigation of the latter case, these modes have been identified and the distribution of the fluctuating components of the fragment angular momenta have been derived.[6]

The angular momentum misalignment can be determined from the angular distributions of particles or photons emitted by one or both fragment, or from the angular distribution of sequential fission fragments. Measurements of angular distributions of sequential alpha particles[7] and gamma rays[8,10] as well as of fission fragments[11-13] have been performed. The analysis of these data requires expressions for the in- and out-of-plane angular distributions, and their specific dependence upon the distributions of the three angular momentum components.

Assuming that these angular momentum distributions are gaussian, we have derived analytical, pocket-size expressions for the angular distributions of sequential light particle emission and fission, specifically accounting for neutron competition effects. The detailed form of the in and out-of-plane angular distributions is discussed.

Similarly, expressions for the angular distributions for the gamma rays both of E1 and E2 multipolarities are derived.

In both cases semiclassical approximations have been adopted. While these expressions are quite general, as they depend only on the Gaussian distribution of the three angular momentum components, it is instructive to apply these equations to a specific model. In particular the results of the statistical model are used to perform calculations for specific reactions and to compare the results with the corresponding experimental data.

Statistical Excitation of Angular Momentum Bearing Modes

Let us consider a frame of reference where the z axis is parallel to the entrance-channel angular momentum, the x axis is parallel to the recoil direction of one of the fragments, and the y axis is perpendicular to the z,x plane.

A misalignment of the fragment angular momentum arises when non-vanishing x and y components of the fragment angular momentum are present. Among the possible sources of these components, the thermal excitation of angular momentum-bearing modes of the intermediate complex appears very likely and can be readily investigated.[6]

If the intermediate complex is assumed to have the shape of two equal touching spheres, the angular momentum bearing normal modes are easily identifiable. In fig. 1 these modes are illustrated. We shall call them "bending," B (doubly degenerate), "twisting" Tw (degenerate with bending), "wriggling" W (doubly degenerate) and "tilting" Ti.

In a recent work, the statistical mechanical aspects of the excitation of these modes has been studied in detail. Here we report only the relevant conclusions.[6]

The thermal excitation of these collective modes leads to Gaussian distributions in the three components I_x, I_y, I_z, namely:

$$P(\underline{I}) \propto \exp - \left[\frac{I_x^2}{2\sigma_x^2} + \frac{I_y^2}{2\sigma_y^2} + \frac{(I_z - \bar{I}_z)^2}{2\sigma_z^2} \right] \qquad (1)$$

where:

$$\sigma_x^2 = \sigma_{Tw}^2 + \sigma_{Ti}^2 = \frac{1}{2}\mathcal{I}T + \frac{7}{10}\mathcal{I}T = \frac{6}{5}\mathcal{I}T$$

$$\sigma_y^2 = \sigma_B^2 + \sigma_w^2 = \frac{1}{2}\mathcal{I}T + \frac{5}{14}\mathcal{I}T = \frac{6}{7}\mathcal{I}T \qquad (2)$$

$$\sigma_z^2 = \sigma_B^2 + \sigma_w^2 = \frac{1}{2}\mathcal{I}T + \frac{5}{14}\mathcal{I}T = \frac{6}{7}\mathcal{I}T \quad .$$

The quantity $\mathcal{I}$ is the moment of inertia of one of the two touching spheres, and T is the temperature.

The assumption of two equal touching spheres is admittedly schematic. However, the generalization to two equal touching spheroids or for that matter to an arbitrary symmetric scission configuration is completely trivial and left to the readers who may have a better idea about the fragment deformation at the scission configuration.

Frequently the degree of alignment of the fragment spins is expressed in terms of the alignment parameter $P_{zz} = 3/2\ \bar{I}_z^2/\bar{I}^2 - 1/2$. If $\sigma_x = \sigma_y = \sigma_z = \sigma$ it is possible to express the alignment parameter P_{zz} in terms of σ and the average z component of the fragment angular momentum $\bar{I}_z$ as follows:

$$P_{zz} = \frac{3}{2}\ \frac{\bar{I}_z^2}{\bar{I}^2} - \frac{1}{2} = \frac{3}{2}\ \frac{\bar{I}_z^2 + \sigma^2}{\bar{I}_z^2 + 3\sigma^2} - \frac{1}{2}$$

Angular Distributions of Sequential Fission and of Sequential Light Particle Emission

The magnitude of the angular momentum misalignment can be measured through the in- and out-of-plane angular distribution of the decay products of one of the two fragments. It has been shown elsewhere that the angular distribution of fission fragments and of light particles emitted by a compound nucleus can be treated within a single framework.[14]

The direction of emission of a decay product (fission fragment, α-particle, etc) is defined by the projection K of the fragment angular momentum on the disintegration axis. Simple statistical mechanical considerations show that the distribution in K values is Gaussian.

Specifically, for any given K, the particle decay width can be written as:

$$\Gamma_K^I \, dK = \Gamma^\circ \exp\left[-\frac{\hbar^2 I^2}{2\mathcal{T}}\left(\frac{1}{\mathcal{J}_\perp} - \frac{1}{\mathcal{J}_c}\right)\right] \exp\left(-\frac{K^2}{2K_o^2}\right)\frac{dK}{I} \qquad (3)$$

where Γ° is an angular momentum independent quantity; T is the temperature; $K_o^2 = \hbar^{-2}(1/\mathcal{J}_\parallel - 1/\mathcal{J}_\perp)^{-1}T$; $\mathcal{J}_\parallel$, $\mathcal{J}_\perp$ are the principal moments of inertia of the decaying system with particle and residual nucleus just in contact, about an axis parallel and perpendicular to the disintegration axis respectively; $\mathcal{J}_c$ is the moment of inertia of the compound nucleus.

Similarly, the neutron decay width, integrated over all the neutron emission directions is

$$\Gamma_N \simeq \Gamma_N^\circ \exp\left[-\frac{\hbar^2 I^2}{2T}\left(\frac{1}{\mathcal{J}_N} - \frac{1}{\mathcal{J}_c}\right)\right] \tag{4}$$

In this expression $\mathcal{J}_N = \mathcal{J}_R + \mu R^2$, corresponding to $\mathcal{J}_\perp$ in eq. (3), is the sum of the moment of inertia of the residual nucleus after neutron decay and the orbital moment of inertia of the neutron at the surface of the nucleus.

Let us now express the particle decay width in terms of the emission angle α measured with respect to the angular momentum direction.

Since $K = I\cos\alpha$ and $dK = Id(\cos\alpha) = Id\Omega$, we obtain:

$$\Gamma^I(\alpha)\, d\Omega = \Gamma^\circ \exp\left[-\frac{\hbar^2 I^2}{2T}\left(\frac{1}{\mathcal{J}_\perp} - \frac{1}{\mathcal{J}_c}\right)\right] \exp -\frac{I^2\cos^2\alpha}{2K_o^2}\, d\Omega$$

If the angular momentum has an arbitrary orientation with respect to our chosen frame of reference, defined by its components I_x, I_y, I_z, the angular distribution can be easily rewritten by noticing that

$$K = I\cos\alpha = \underset{\sim}{I}\cdot\underset{\sim}{n} = I_x\sin\theta\cos\phi + I_y\sin\theta\sin\phi + I_z\cos\theta$$

where $\underset{\sim}{n}$ is a unit vector pointing the direction of particle emission with polar angles θ,ϕ. If the orientation of the angular momentum is controlled by the distribution

$$P(\underline{I}) \propto \exp - \left[\frac{I_x^2}{2\sigma_x^2} + \frac{I_y^2}{2\sigma_y^2} + \frac{(I_z - \bar{I}_z)^2}{2\sigma_z^2} \right] \tag{6}$$

we can integrate over the distribution of orientations and we obtain, dropping angular momentum independent factors:[16]

$$\Gamma^I(\theta,\phi)\, d\Omega \propto \exp\left[- \frac{\hbar^2 I^2}{2T} \left(\frac{1}{\mathcal{J}_\perp} - \frac{1}{\mathcal{J}_c} \right) \right] \frac{1}{S(\theta,\phi)} \exp - \frac{I^2 \cos^2\theta}{2S^2(\theta,\phi)}\, d\Omega \tag{7}$$

where:

$$S^2(\theta,\phi) = K_o^2 + (\sigma_x^2 \cos^2\phi + \sigma_y^2 \sin^2\phi) \sin^2\theta + \sigma_z^2 \cos^2\theta \tag{8}$$

In the above expression (7) we have set $I_z = I$, in other words we have averaged over the orientation but we have allowed the decay width to depend only upon the average angular momentum set equal to its z component. This expression should then be considered only as a high angular momentum limit ($\sigma/I << 1$).

The final angular distribution is obtained by integration over the fragment angular momentum distribution which we assume to reflect the entrance channel angular momentum distribution through the rigid rotation condition:

$$\frac{d\sigma}{d\Omega} \propto \int_{I_{min}}^{I_{mx}} 2I\, dI\, \frac{\Gamma^I}{\Gamma_N} \tag{9}$$

where we have made the frequently valid approximation $\Gamma_T \approx \Gamma_N$.

More precisely:

$$W(\theta,\phi) \propto \int_{I_{min}}^{I_{mx}} \frac{2I}{S} \exp\left[-I^2\left(\frac{\cos^2\theta}{2S^2} - \beta\right)\right] dI \tag{10}$$

or

$$W(\theta,\phi) = \frac{1}{S}\left[\frac{I_{min}^2}{A_{min}} \exp(-A_{min}) - \frac{I_{min}^2}{A_{mx}} \exp(-A_{mx})\right] \tag{11}$$

If $I_{min} = 0$, then:

$$W(\theta,\phi) = \frac{1}{SA}\left[1 - \exp(-A)\right]$$

where

$$A = A_{mx} = I_{mx}^2\left[\frac{\cos^2\theta}{2S^2} - \beta\right] \; ; \quad A_{min} = I_{min}^2\left[\frac{\cos^2\phi}{2S^2} - \beta\right] \tag{12}$$

$$\beta = \frac{\hbar^2}{2T}\left(\frac{1}{\mathcal{J}_n} - \frac{1}{\mathcal{J}_\perp}\right)$$

The quantity $\mathcal{J}_n$ is the moment of inertia of the nucleus after neutron emission, $\mathcal{J}_\perp$ is the perpendicular moment of inertia of the critical shape for the decay (e.g., saddle point).[14]

It is important to notice that the angular momentum dependence of the particle/neutron competition or fission/neutron competition is explicitly taken into account through β. This point seems to have been neglected in recent work on sequential decay.

The final ingredient necessary for an explicit calculation of the angular distributions is the quantity K_o^2. This quantity can be expressed in terms of the principal moments of inertia of the critical configuration for the decay:

$$K_o^2 = \frac{1}{\hbar^2}\left(\frac{1}{\mathcal{J}_{\parallel}} - \frac{1}{\mathcal{J}_{\perp}}\right)^{-1} T = \mathcal{J}_{eff} T \tag{13}$$

For fission $\mathcal{J}_{eff}$ can be taken from the liquid drop calculations.[16] For lighter particle emission, the calculation of $\mathcal{J}_{eff}$ can be worked out trivially. Let m, M, A be the masses of the light, residual and total nucleus. One obtains:

$$\mathcal{J}_{\parallel} = \frac{2}{5} MR^2 + \frac{2}{5} mr^2$$

$$\mathcal{J}_{\perp} = \frac{2}{5} MR^2 + \frac{mM}{A}(R + r)^2 \tag{14}$$

$$\frac{\mathcal{J}_{eff}}{\mathcal{J}_{sph}} = \left(\frac{M}{A}\right)^{5/3}\left[1 + \frac{2}{5}\,\frac{A}{m}\left(\frac{R}{R + r}\right)^2\right]$$

where r and R are the radii of the light particle and residual nucleus respectively.

This result is adequate if m << M and if the charge of the light particle is small. If the charge of the light particle is not negligible, one has to consider the shape polarization induced on the heavy fragment at the ridge point, as discussed in ref. 14. Since the shape polarization affects the asymptotic kinetic energy of the emitted particle as well, one can in principle utilize the particle kinetic energy spectra to verify that the shape of the system at the ridge point and its principal moments of inertia have been properly chosen.[7] Again a more complete discussion on this point is available in ref. 14.

Calculations of sequential fission angular distributions performed with a special combination of semiclassical and quantum mechanical approaches are described in ref. 17. In these calculations no neutron competition is accounted for, nor angular momentum fluctuations about the z axis. We shall point out the effect of neglecting these aspects of the problem later-on.

Now we are in the position to calculate both in-plane and out-of-plane anisotropies.

The in plane anisotropy gives:

$$\left.\frac{W(\phi = 90^\circ)}{W(\phi = 0^\circ)}\right|_{\theta=90^\circ} = \left(\frac{K_0^2 + \sigma_x^2}{K_0^2 + \sigma_y^2}\right)^{1/2} \tag{15}$$

Since in most cases K_0^2 is fairly large, or at least comparable with σ_x^2 or σ_y^2, it is difficult to obtain a sizable in-plane anisotropy. Even by letting $\sigma_x = 0$ one needs $\sigma_y^2 = 3\ K_0^2$ just to obtain the anisotropy of 2! The out-of-plane anisotropy is somewhat more complicated: For a fixed angular momentum I one has:

$$\left.\frac{W(\theta = 90^\circ)}{W(\theta = 0^\circ)}\right|_{\phi=0^\circ} = \left(\frac{K_0^2 + \sigma_z^2}{K_0^2 + \sigma_x^2}\right)^{1/2} \exp\left(\frac{I^2}{2(K_0^2 + \sigma_z^2)}\right) \quad .$$

For the usual angular momentum distribution one obtaines:

$$\left.\frac{W(\theta = 90^\circ)}{W(\theta = 0^\circ)}\right|_{\phi=0^\circ} = \frac{1}{\beta}\left(\frac{K_o^2 + \sigma_z^2}{K_o^2 + \sigma_x^2}\right)^{1/2} \left(\beta - \frac{1}{2(K_o^2 + \sigma_z^2)}\right)$$

$$\times \frac{1 - \exp \beta I_{mx}^2}{1 - \exp I_{mx}^2 \left(\beta - \frac{1}{2(K_o^2 + \sigma_z^2)}\right)}$$

At $\phi = 90^\circ$ the anisotropy is obtained from the above equations by interchanging σ_x with σ_y.

Some Calculations for Sequential Fission and Alpha Decay and Comparison with Data

The results obtained above can be illustrated by applying them to a reaction which has been experimentally investigated. We choose the reaction 600 MeV ^{86}Kr + Au.[11] For this reaction we estimate $\mathcal{J}_{sph}/\mathcal{J}_{eff} = 1.864$, $K_o^2 = 100\ \hbar^2$, $\beta = 0.00194\ \hbar^{-2}$, $I_{mx} = 40\hbar$, $\sigma^2 \simeq 110\ \hbar^2$. In order to simultaneously appreciate the shapes of the in- and out-of-plane angular distributions possible in sequential fission, we have artificially set $\sigma_x^2 = 0$, $\sigma_y^2 = \sigma_z^2 = 110\ \hbar^2$. The results are shown in fig. 2. In this figure one readily appreciates the connection between the in-plane and the out-of-plane angular distributions. In particular, it is apparent how an in-plane anisotropy

must necessarily be associated with a variation of the out-of-plane width with the in-plane angle.

We have stressed already that the competition between fission and neutron decay must be dealt with specifically because of the strong dependence of Γ_F upon angular momentum. This is illustrated in fig. 3 where we have set $\sigma_x^2 = \sigma_y^2 = \sigma_z^2 = 110\ \hbar^2$ and we have assumed $\beta = 0.00194\ \hbar^{-2}$ in one case, and $0.000\ \hbar^{-2}$ in the other. The effect is quite dramatic, and clearly must be incorporated in the formalism if one intends to obtain reliable angular momentum values from it. For instance, in order to compensate for setting $\beta = 0.000$ instead of $0.00194\ \hbar^{-2}$ it is necessary to step-up the angular momentum I_{mx} from 40 to 55 $\hbar$.

The predicted FWHM = 54° can be compared with the data[11] shown in fig. 4. The agreement is quite satisfactory.

The present calculations can be compared to those in ref. 17 where no angular momentum distribution is assumed and thus no neutron competition is included. In the same work no fluctuation in the z component of angular momentum is allowed. Neglection of σ_z ($\sigma_z = 0$) cannot be directly translated into a variation in the angular momentum, because of the difference in the functional dependence. However, a decrease of I_{mx} from $I_{mx} = 40\ \hbar$ to $I_{mx} = 34\ \hbar$ approximately compensates for setting $\sigma_z = 0$. This range of more than 20 $\hbar$ illustrates how dependent is the inferred fragment angular momentum upon the inclusion of angular momentum fluctuations about the z axis and upon the inclusion of neutron competition. Extreme caution is obviously in

order when the extracted angular momenta are compared with theoretical predictions, like the rigid rotation limit.

In the same spirit as for sequential fission we show some calculations for sequential alpha decay in the reaction 664 MeV ^{84}Kr + Ag. The alpha particles are assumed to be emitted by the Ag-like nucleus. We estimate $I_{mx} = 36\ \hbar$, $\sigma^2 = 68\ \hbar^2$, $\beta = 0.00137\ \hbar^{-2}$ and $K_o^2 = 365\ \hbar^2$. The results are shown in fig. 5. For comparison a calculation with $\sigma^2 = 0$ is also shown in order to illustrate the sensitivity to misalignment. Examples of fits to experimental data[7] are shown in fig. 6. From these data it is possible to infer the dependence of the heavy fragment spin upon mass asymmetry. It is observed that its value is close to that of rigid rotation (fig. 7).

Gamma ray angular distributions

Fragments with large amounts of angular momentum are expected to dispose of it mainly by stretched E2 decay. The relative amounts of dipole and quadrupole radiation depend mainly upon the ability of the nucleus to remain a good rotor over the whole angular momentum range.

If the angular momentum of the fragment is aligned, the typical angular pattern of the quadrupole radiation should be observed. Any misalignment should decrease the sharpness of the angular distribution.

If the distribution of the angular momentum components I_x, I_y, I_z is statistical, it is straightforward to derive analytical expressions for the angular distributions.

For a perfectly aligned system we have:

$$W(\alpha) = \frac{3}{4}(1 + \cos^2\alpha) \quad ; \quad W(\alpha) = \frac{5}{4}(1 - \cos^4\alpha) \tag{17}$$

for E1 for E2

If the angular momentum is not aligned with the z axis, one must express α in terms of θ, ϕ which define the direction of the angular momentum vector. In particular we have:

$$\cos\alpha = \frac{\underset{\sim}{I}\cdot\underset{\sim}{n}}{I} = \frac{I_x \sin\theta\cos\phi + I_y \sin\theta\sin\phi + I_z\cos\theta}{(I_x^2 + I_y^2 + I_z^2)^{1/2}} \tag{18}$$

It is to be noticed, at this stage, that we assume the angular momentum to behave as a classical vector. For any given I, the angular distribution is obtained by integration over the statistical distribution $P(\underset{\sim}{I})$ of the angular momentum components:

$$W(\theta,\phi) = \int W(\alpha)\, P(\underset{\sim}{I})\, d\underset{\sim}{I} \tag{19}$$

It is not possible to obtain exact analytical expression for the general case. However, an expansion to order $\sigma_x^2/\bar{I}_z^2$, $\sigma_y^2/\bar{I}_z^2$, etc. allows one to obtain expressions in closed form.

For the dipole decay we have:

$$W(\theta,\phi) = \frac{3}{4}(1 + \cos^2\theta) + \frac{3}{4}\left[(\sin^2\theta\cos^2\phi - \cos^2\theta)\frac{\sigma_x^2}{\bar{I}_z^2} + (\sin^2\theta\sin^2\phi - \cos^2\theta)\frac{\sigma_y^2}{\bar{I}_z^2}\right] \tag{20}$$

Notice that there is no dependence upon σ_z^2. In the case in which $\sigma_x = \sigma_y = \sigma$, we obtain the simplified expression:

$$W(\theta,\phi) = \frac{3}{4}(1 + \cos^2\theta) + \frac{3}{4}(\sin^2\theta - 2\cos^2\theta)\frac{\sigma^2}{\bar{I}_z^2} \tag{21}$$

A weak in-plane anisotropy is possible:

$$\left.\frac{W(\phi = 0^\circ)}{W(\phi = 90^\circ)}\right|_{\theta=90^\circ} = \frac{1 + \sigma_x^2/\bar{I}_z^2}{1 + \sigma_y^2/\bar{I}_z^2} \cong 1 + \frac{\sigma_x^2 - \sigma_y^2}{\bar{I}_z^2} \tag{22}$$

The out-of-plane anisotropy is:

$$\frac{W(0^\circ)}{W(90^\circ)} = 2\frac{(1 - \sigma^2/\bar{I}_z^2)}{(I + \sigma^2/\bar{I}_z^2)} \cong 2(1 - 2\sigma^2/\bar{I}_z^2) \tag{23}$$

For the quadrupole decay we have:

$$W(\theta,\phi) = \frac{5}{4}\,(1 - \cos^4\theta) - \frac{5}{2}\left[(3\,\sin^2\theta\,\cos^2\theta\,\cos^2\phi - \cos^4\theta)\,\frac{\sigma_x^2}{\bar{I}_z^2}\right.$$

$$\left. + (3\sin^2\theta\,\cos^2\theta\,\sin^2\phi - \cos^4\theta)\,\frac{\sigma_y^2}{\bar{I}_z^2}\right] \qquad (24)$$

Again, no dependence upon σ_z^2 is predicted. If one assumes $\sigma_x = \sigma_y = \sigma$ as before, one obtains:

$$W(\theta) = \frac{5}{4}\,(1 - \cos^4\theta) - \frac{5}{2}\,(3\sin^2\theta\,\cos^2\theta - 2\cos^4\theta)\,\sigma^2/\bar{I}_z^2 \qquad (25)$$

and

$$\frac{W(0^\circ)}{W(90^\circ)} \simeq 4\,\frac{\sigma^2}{\bar{I}_z^2} \qquad (26)$$

For the in plane anisotropy we have:

$$\left.\frac{W(\phi = 0^\circ)}{W(\phi = 90^\circ)}\right|_{\theta=90^\circ} \sim 1 \qquad (27)$$

to order $\sigma^2/\bar{I}_z^2$. This can be easily understood. The rms misalignment is $\sim\sigma/I$, thus, at $\theta = 90^\circ$:

$$W(90) = 1 - \cos^4\left(90^\circ - \frac{\sigma}{I}\right) \simeq 1 - \frac{\sigma^4}{I^4}$$

Thus, no second order term exists. This result shows that its is very difficult to study anisotropies in the angular momentum misalignment by means of γ-ray angular distribution.

The range of validity of the above expressions is rather limited due to the low order expansion. In particular, the equations should not be trusted for $\sigma^2/\bar{I}_z^2 > 0.05$.

However, if we are willing to assume $\sigma_x^2 = \sigma_y^2 = \sigma_z^2 = \sigma$ then an exact result can be obtained.

For the E1 distribution one obtains:

$$W(\theta)_{E1} = \frac{3}{4}\left[1 + \cos^2\theta + \lambda^2(1 - D(\lambda))(1 - 3\cos^2\theta)\right] \tag{28}$$

For the E2 distribution one obtains:

$$\begin{aligned} W(\theta)_{E2} = \frac{5}{4}\Big[1 - \cos^4\theta - 2\lambda^2 \Big\{ & 3\sin^2\theta\cos^2\theta - 2\cos^4\theta + \\ & - \frac{3}{4} D(\lambda)(\sin^2\theta - 4\cos^2\theta)\sin^2\theta \Big\} + \\ & - 3\lambda^4 \Big\{ 4\cos^4\theta + \frac{3}{2}\sin^4\theta - 12\sin^2\theta\cos^2\theta \Big\}(1 - D(\lambda))\Big] \end{aligned} \tag{29}$$

In these equations $\lambda = \sigma/\bar{I}_z$ and $D(\lambda) = \sqrt{2}\,\lambda\, F(1/\sqrt{2}\,\lambda)$ where

$$F(x) = e^{-x^2}\int_0^x e^{t^2} dt$$

is the Dawson's integral. One can verify immediately that both expressions behave as expected in the limits of $\lambda = 0$ and $\lambda = \infty$. In fig. 8 one can verify that the anisotropy $W(0)/W(90^\circ)$ tends to 1 when λ tends to infinity both for E1 and E2 transitions, while it tends to 0 for E2 and to 2 for E1 when $\lambda = 0$.

For convenience of calculations, we give here an expansion of these equations up to 8^{th} order in λ which is adequate up to $\lambda^2 \leq 0.4$

For E_1 we obtain:

$$W(\theta) \simeq \frac{3}{4}\left[1 + \cos^2\theta + \lambda^2(1 - 3\cos^2\theta) - \lambda^4(1 - 3\cos^2\theta) - \lambda^6(1 - 3\cos^2\theta) - 3\lambda^8(1 - 3\cos^2\theta)\right] \tag{30}$$

$$\frac{W(0^\circ)}{W(90^\circ)} \simeq \frac{2 - 2\lambda^2 + 2\lambda^4 + 2\lambda^6 + 6\lambda^8}{1 + \lambda^2 - \lambda^4 - \lambda^6 - 3\lambda^8}$$

Similarly, for E2 we obtain:

$$W(\theta)_{E2} \simeq \frac{5}{4}\left[1 - \cos^4\theta - 2\lambda^2\left\{3\sin^2\theta\cdot\cos^2\theta - 2\cos^4\theta\right\} - 3\lambda^4\left\{4\cos^4\theta + \sin^4\theta - 10\sin^2\theta\cos^2\theta\right\} + 6\lambda^6\left\{2\cos^4\theta + \sin^4\theta - 7\sin^2\theta\cos^2\theta\right\} + 3\lambda^8\left\{3\sin^4\theta + 4\cos^4\theta - 18\sin^2\theta\cos^2\theta\right\}\right] \tag{31}$$

$$\frac{W(0^\circ)}{W(90^\circ)} \simeq \frac{4\lambda^2(1 - 3\lambda^2 + 3\lambda^4 + 3\lambda^6)}{(1 - 3\lambda^4 + 6\lambda^6 + 9\lambda^8)}$$

It is recommended that these last equations be used instead of eqs. (21, 23, 25 and 27) in actual calculations.

These results are graphically summarized in fig. 9 where the anisotropy is plotted as a function of the fraction of E1 radiation for various values of $\sigma^2/\bar{I}^2$. The two extreme possibilities of stretched and non-stretched E1 decay are considered. If one has a fairly good experimental idea of the amount of E1 radiation to be expected from a given fragment and of its degree of stretching, the measurement of the anisotropy yields directly the value of $\sigma^2/\bar{I}^2$, which is of course the most direct information about the misalignment.

It goes without saying that if one is to deal with a distribution of fragment spins, the angular distribution associated with each spin I should be weighted by a factor proportional to I in order to account for the fact that each nucleus with spin I emits about I/2 gamma rays all with essentially the same angular distribution.

Application to Experimental γ-Ray Angular Distributions

An interesting measurement has been carried out for the reaction[10] 1400 MeV ^{165}Ho + ^{165}Ho. This system was chosen because large amounts of angular momentum can be transferred into the intrinsic spin (I) of these nuclei, which are known to have good rotational properties. As a consequence, both of the essentially identical DI-fragments emit similar continuum γ-ray spectra which are strongly enriched in E2 transitions (~80 percent).

Figure 10(a) shows the fragments' energy spectrum obtained at an angle slightly greater than the grazing angle. Figure 10(b) shows the

intrinsic spin of one of the two reaction fragments after neutron emission (circles). The primary fragment spin obtained from M_γ with correction for neutron emission (solid line) is also shown.

The ratio of in-plane to out-of-plane γ-ray yield ("anisotropy") for energies between 0.6 and 1.2 MeV (squares) is shown in fig. 2(b). This anisotropy rises with increasing spin transfer; it peaks at a value of ~2.2, slightly before the spin saturates, and then drops to near unity for large Q-values. Figure 2(c) shows the dependence of the anisotropy on both E_γ and Q in two-dimensional contour diagram.

The initial rise of anisotropy with increasing Q-value indicates that during the early stages of energy damping there is a rapid buildup of aligned spin. The subsequent fall observed at larger Q-values suggests that the aligned component of spin has saturated or is decreasing, whereas randomly-oriented components continue to increase, causing a significant decrease in the alignment of the fragments' spin.

Figure 11(a) shows experimental values of the anisotropy for E_γ greater than 0.3 MeV compared to several stages of the model calculation. The spin I was determined from the γ-ray multiplicity, and the anisotropy was then calculated (fig. 11(a)), solid line). This calculation reproduces both the shape and the magnitude of the data. To give a feeling for the importance of various contributions, the same calculation is shown with no correction for neutron evaporation (curve 2), assuming no statistical transitions (curve 3), and with no thermal effects (curve 4). This comparison clearly shows that the most

important effect is the thermally induced misalignment, indicating that the decrease of alignment as deduced from the anisotropy is inherent to the deep-inelastic process itself.

By gating on the 0.6-1.2 MeV region of the E_γ spectra, one both increases the fraction of E2-transitions and biases the spin distribution to larger values, which should yield larger anisotropies. In fig. 11(b), measured (symbols) and calculated (solid line) anisotropies are shown for the 0.6-1.2 MeV γ-ray region. These data show the expected larger anisotropies, which the model calculations reproduce.

Summary

The purpose of this paper has been to provide general, easy and simple to use expressions for the angular distributions of particles and gamma-rays emitted by deep inelastic fragments. The models used in deriving the various equations are semiclassical and the assumed distributions for the angular momentum compounds are Gaussians. This combination of features has allowed us to obtain analytical expressions which are expected to be valid in most cases and whose physics is quite transparent.

References

1. For general reference see for instance:
L. G. Moretto and R. Schmitt, J. Phys. 37, C5-109 (1976); M. Lefort and C. Ngô, Riv. Nuovo Cimento 12, 1 (1979).
2. R. Reginbart, A. Behkami, G. J. Wozniak, R. P. Schmitt, J. J. Sventek and L. G. Moretto, Phys. Rev. Lett. 41, 1355 (1978).
3. M. M. Aleonard, G. J. Wozniak, P. Glässel, M. M. Deleplanque, R. M. Diamond, L. G. Moretto, R. P. Schmitt and F. S. Stephens, Phys. Rev. Lett. 40, 622 (1978).
4. P. Glässel, R. S. Simon, R. M. Diamond, R. C. Jared, I. Y. Lee, L. G. Moretto, J. O. Newton, R. Schmitt and F. Stephens, Phys. Rev. Lett. 38, 331 (1977).
5. J. B. Natowitz, N. M. Namboodiri, P. Kasiraj, R. Eggers, L. Adler, P. Goutier, C. Cerutti and T. Alleman, Phys. Rev. Lett. 40, 751 (1978).
6. L. G. Moretto and R. P. Schmitt, Phys. Rev. C21, 204 (1980).
7. L. G. Sobotka, G. C. Hsu, G. S. Wozniak, G. U. Rattazzi, R. J. McDonald, A. Pacheco and L. G. Moretto, LBL-11148.
8. H. Puchta, W. Dunnweber, H. Hering, L. Lauterbach and W. Trautmann, Phys. Rev. Lett. 43, 623 (1979).
9. P. Aguer, G. J. Wozniak, R. P. Schmitt, D. Habs, R. M. Diamond, C. Ellegard, D. Hillis, C. C. Hsu, G. J. Mathews, L. G. Moretto, G. U. Rattazzi, C. P. Roulet, and F. Stephens, Phys. Rev. Lett. 43, 1778 (1979).

10. G. J. Wozniak, R. J. McDonald, A. Pacheco, C. C. Hsu, D. J. Morrissey, L. G. Sobotka, L. G. Moretto, S. Shih, C. Schuck, R. M. Diamond, H. Klüge and F. S. Stephens, Phys. Rev. Lett. 45, 1081 (1980).

11. G. J. Wozniak, R. P. Schmitt, P. Glässel, R. C. Jared, G. Bizard, and L. G. Moretto, Phys. Rev. Lett. 40, 1436 (1978).

12. P. Dyer, R. J. Puigh, R. Vandenbosch, T. D. Thomas, M. S. Zisman and L. Nunnely, Nucl. Phys. A322, 205 (1979).

13. H. Specht, Lecture Notes in Physics 92, 1, 1979, ed. B. A. Robson.

14. L. G. Moretto, Nucl. Phys. A247, 211 (1975).

15. R. A. Broglia, G. Pollarolo, C. H. Dasso and T. Dössing, Phys. Rev. Lett. 43, 1649 (1979).

16. S. Cohen, F. Plasil and W. S. Swiatecki, Ann. Phys. 82, 557 (1974).

17. B. B. Back and S. Bjørnholm, Nucl. Phys. A302, 343 (1978).

Figure Captions

Fig. 1. (a) A pictorial description of the tilting mode and of the doubly degenerate wriggling modes for the two equal sphere model. The arrow originating at the point of tangency represents the orbital angular momentum while the shorter arrows represent the individual fragment spins.
(b) A pictorial illustration of the twisting and bending modes for the two equal sphere model. Note the pairwise cancellation of the fragment spins.

Fig. 2. Calculated in-plane (dashed line) and out-of-plane (solid lines) angular distributions for sequential fission fragments in the reaction 60 MeV Kr + Au. The in-plane anisotropy is artifically generated by setting $\sigma_x = 0$.

Fig. 3. Calculated sequential fission angular distributions for the system 600 MeV Kr + Au. The curve labeled $\beta = 0.0$ corresponds to disregarding neutron emission fission competition. The more realistic curve labeled $\beta = 0.00194$ gives a FWHM of 54°.

Fig. 4. Experimental full width at half maximum of the out-of-plane angular distribution for fission and non-fission components as a function of Z in the reaction 618 MeV ^{86}Kr + ^{197}Au.[11] The squares represent the data in the lab system, the triangles the data in the center of mass of the Au-like fragment. The dots represent the non fissioning Au-like recoils.

Fig. 5. Calculated out-of-plane angular distribution for sequential alpha decay from the Ag-like fragment in the reaction 664 MeV $^{84}Kr + ^{nat}Ag$ (dashed line.[7] The solid line has been obtained by setting $\sigma = 0$.

Fig. 6. Experimental alpha particle angular distributions for several Z-bins as a function of out-of-plane angle for the same reaction as in Fig. 5. The Z bins are 3 Z's wide and are indicated by the median Z. In Section (a) there is no coincident γ-ray requirement while in (b) there are 2 or more coincident γ-rays. The curves in section (b) are normalized at 90° to those in (a) for the same Z bin.

Fig. 7. Average heavy fragment spin as a function of the light fragment atomic number. The dots represent the spins extracted from data without γ-ray coincidence requirement. The open circles represent the spins obtained when 2 or more γ-rays are required in coincidence. The line represents the rigid rotation limit for two equally deformed spheroids with ratio of axis 2:1.[7]

Fig. 8. (a) Dependence of the gamma-ray anisotropy upon $\sigma^2/\bar{I}_Z^2$ for a mixture of stretched E2 and E1 transitions (see text). (b) Same as in 8(a), but for a mixture of random E1 and stretched E2.

Fig. 9. (a) Gamma-ray anisotropy for a mixture of stretched E1 and E2 transitions as a function of the fraction of E1 radiation for various values of $\sigma^2/\bar{I}_Z^2$.

Fig. 10. (a) Q-value spectrum for the $^{165}Ho + ^{165}Ho$ reaction[10] at 27° in the laboratory.

(b) Post- (circles) and pre(solid line) neutron emission values of the spin per fragment $\langle I_1 \rangle$ as a function of the reaction Q-value. The anisotropies, $W(in/\perp)$, are also shown (squares) for the E_γ region 0.6-1.2 MeV.

(c) Anisotropy contours for coordinates E_γ and Q.

Fig. 11. Experimental (symbols) and calculated (curves) values of the anisotropy, $W(in/\perp)$, (a) for γ-rays greater than 0.3 MeV and (b) for the region 0.6 MeV < E_γ < 1.2 MeV. In part (a) curve 2 disregards neutron evaporation, curve 3 assumes no statistical E1 transitions, and curve 4 disregards the thermal excitation of angular momentum bearing modes. The latter effect is dominant in determining the magnitude and Q-value dependence of the anisotropy.

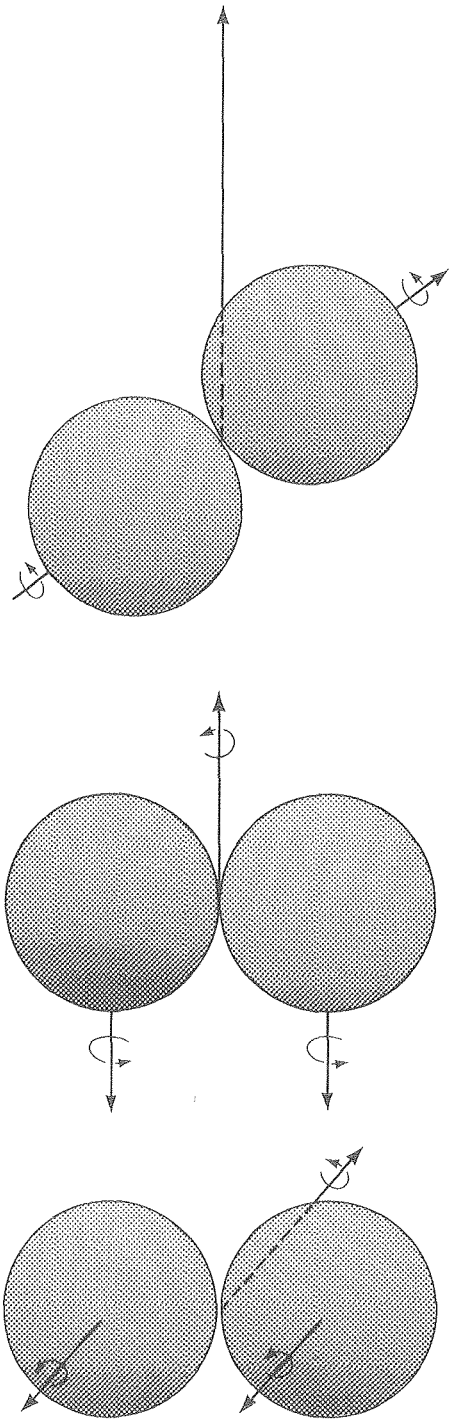

Fig. 1a

XBL 793-824

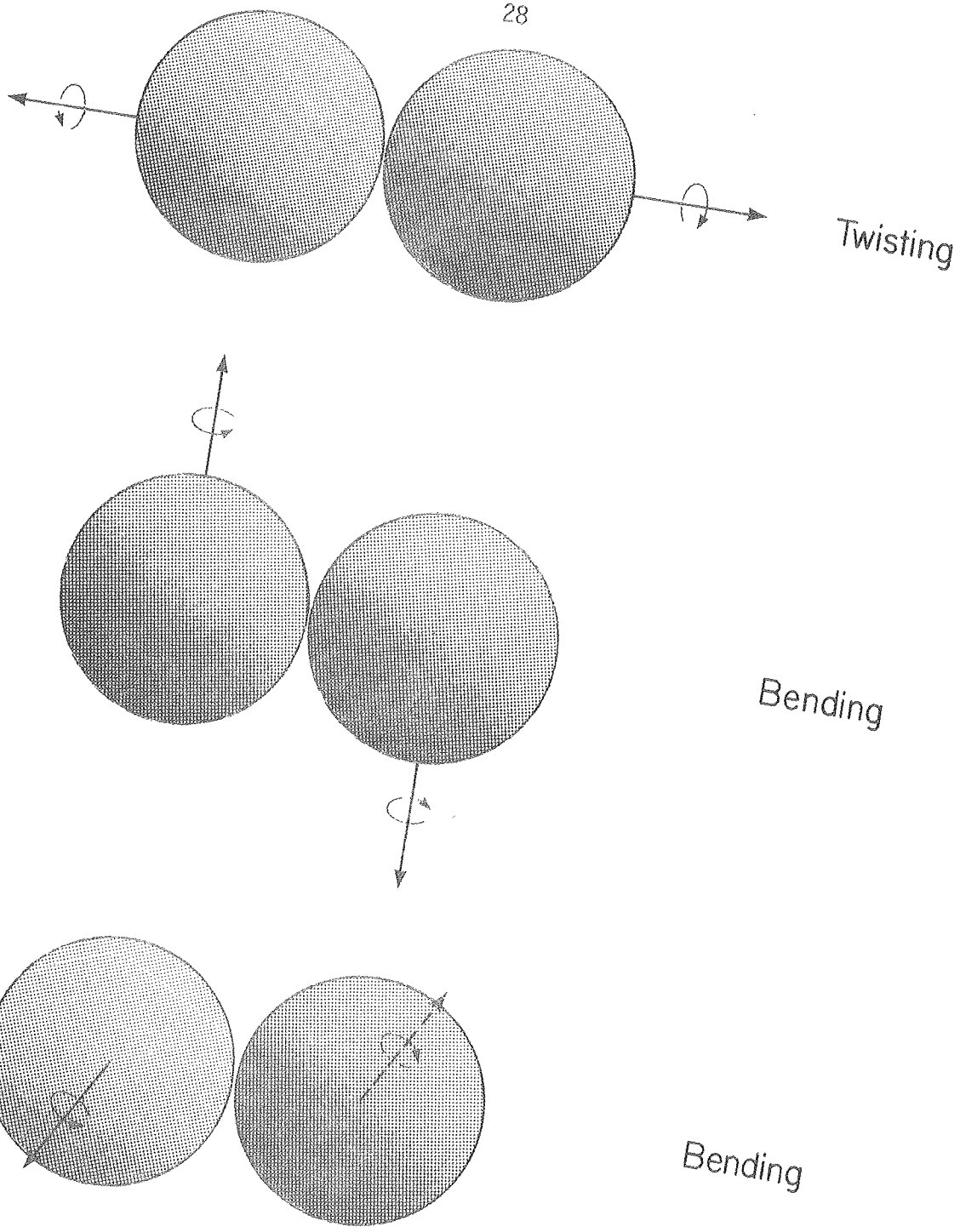

Fig. 1b

XBL 791-206

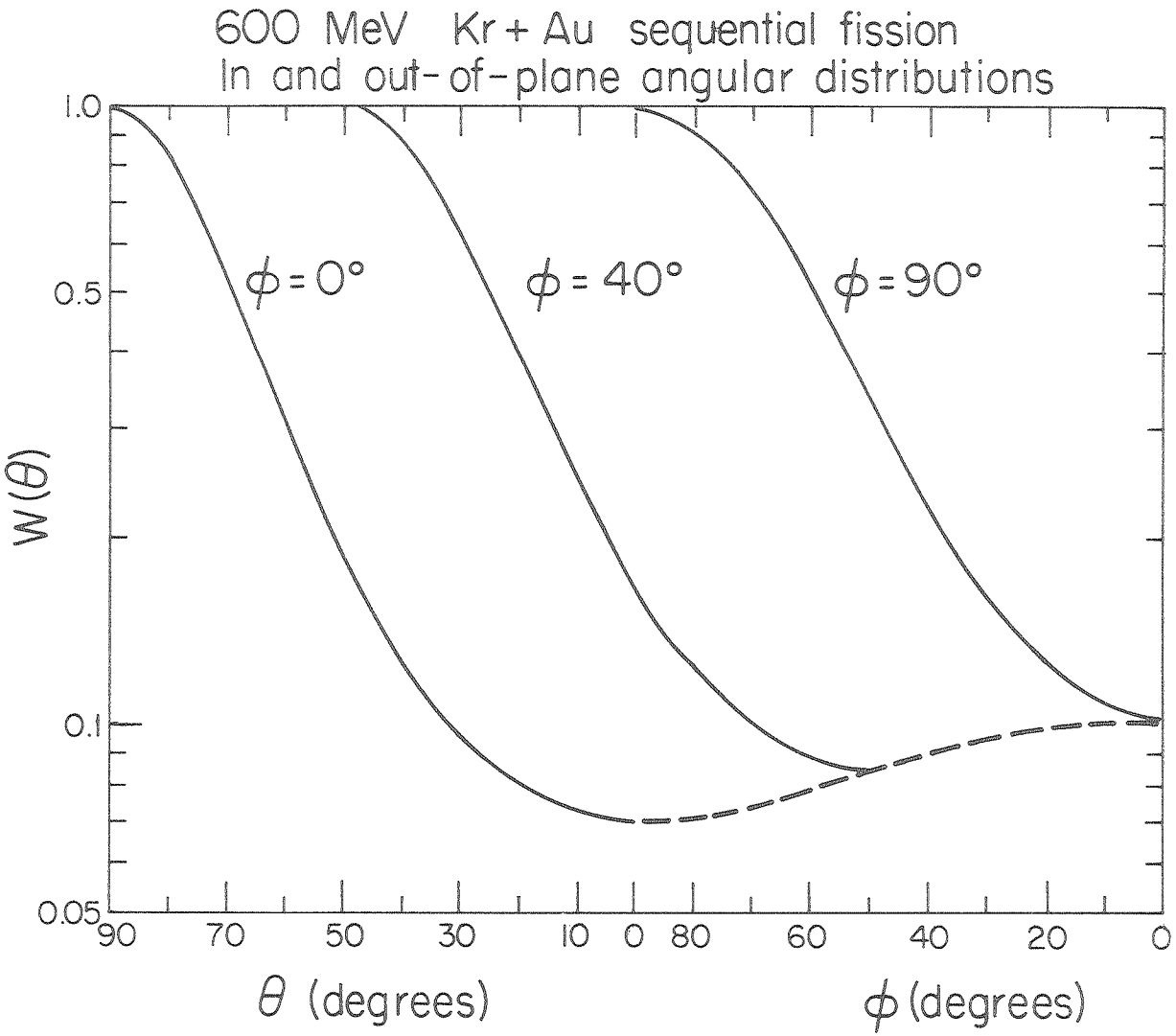

Fig. 2

XBL 802-277

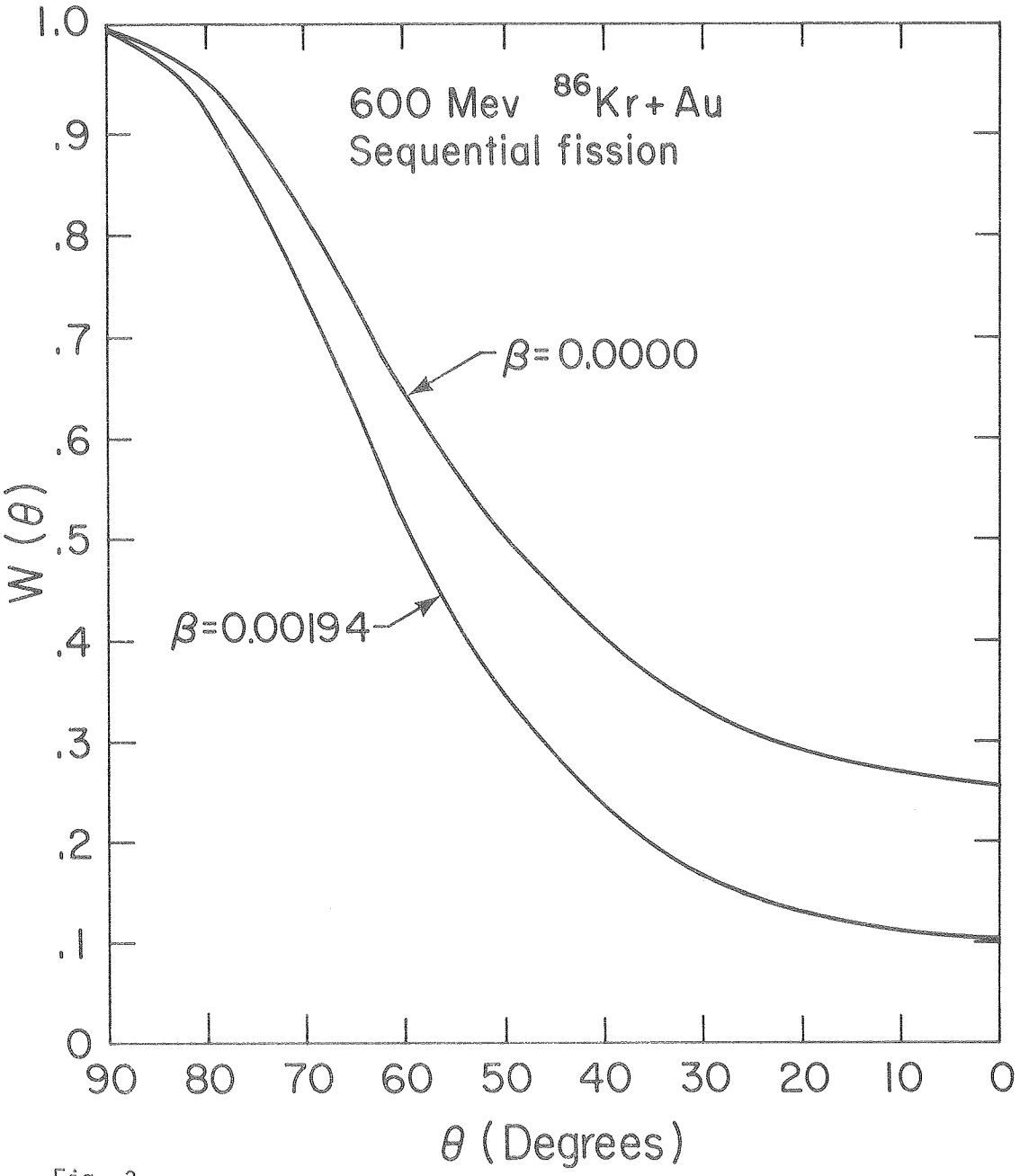

Fig. 3

XBL 807-1672

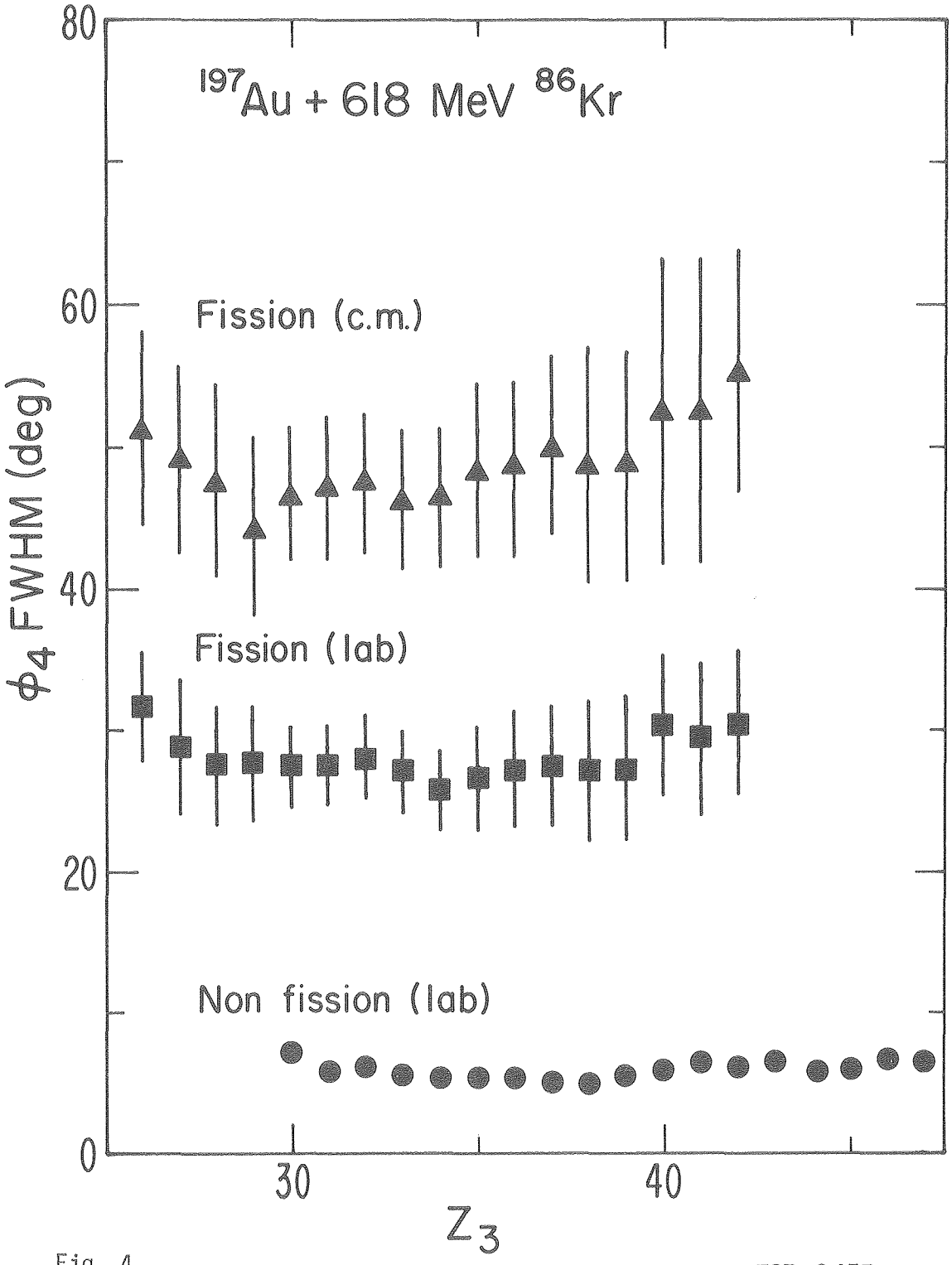

Fig. 4

XBL 783-2453

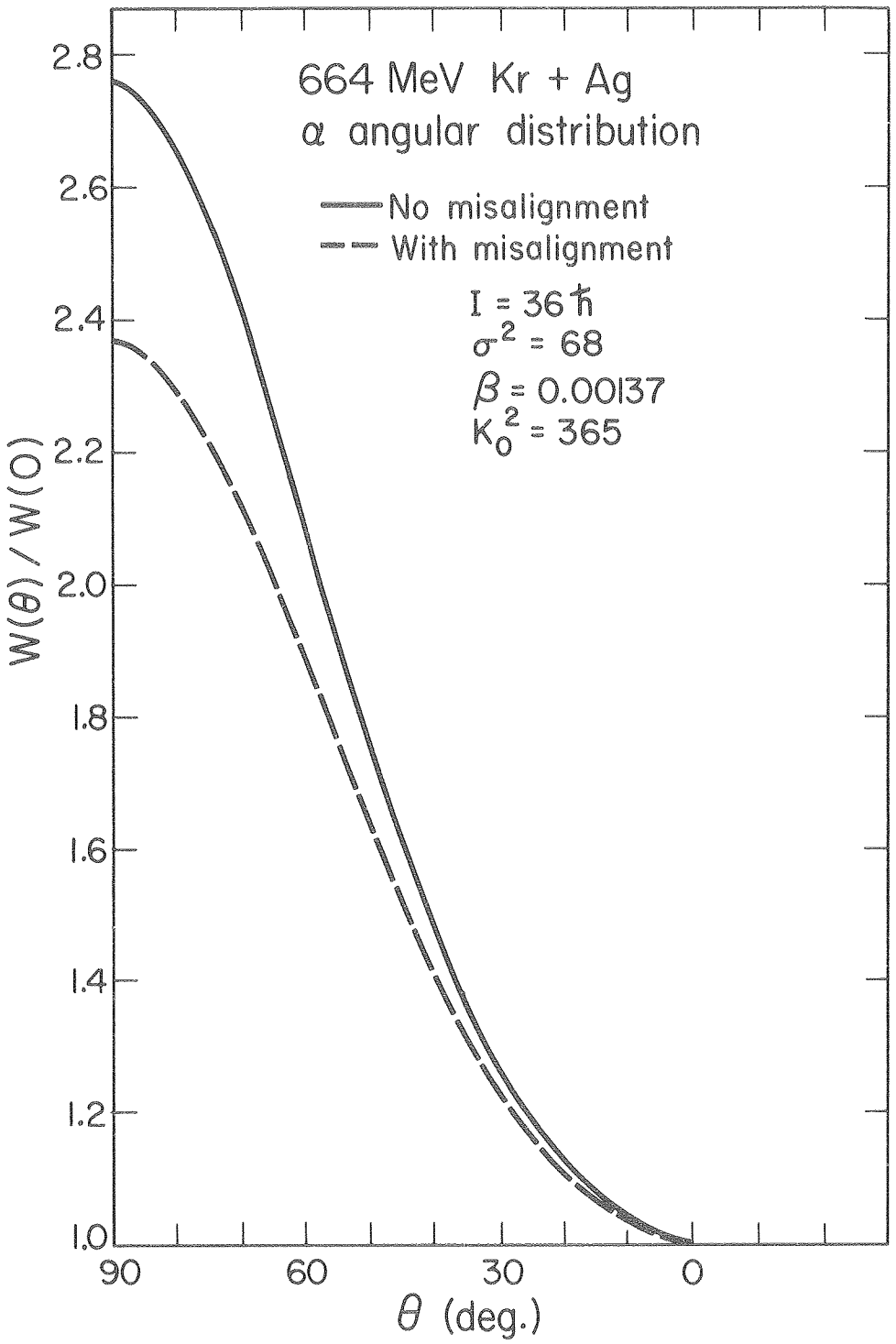

Fig. 5

XBL 802-285

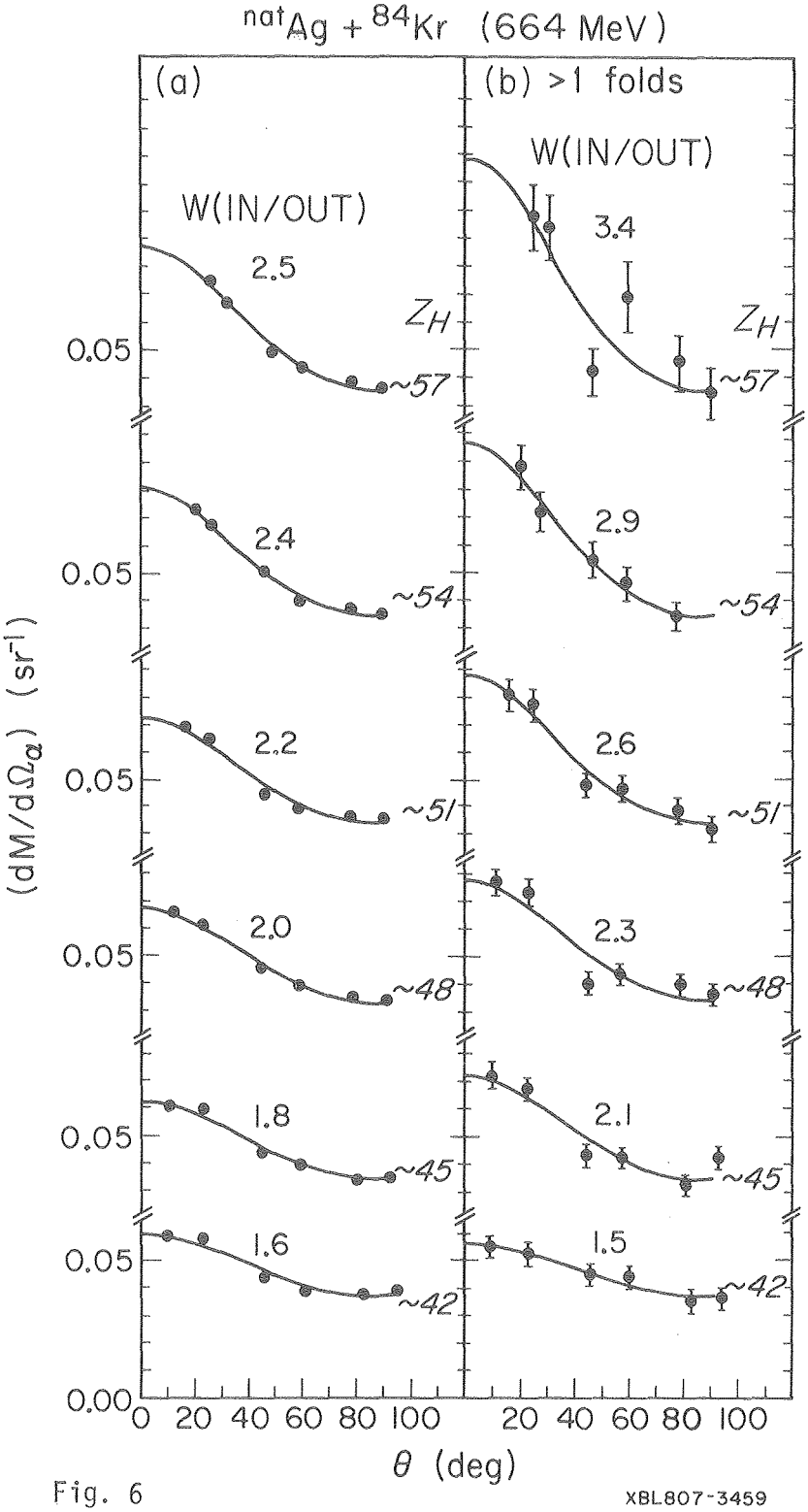

Fig. 6

XBL807-3459

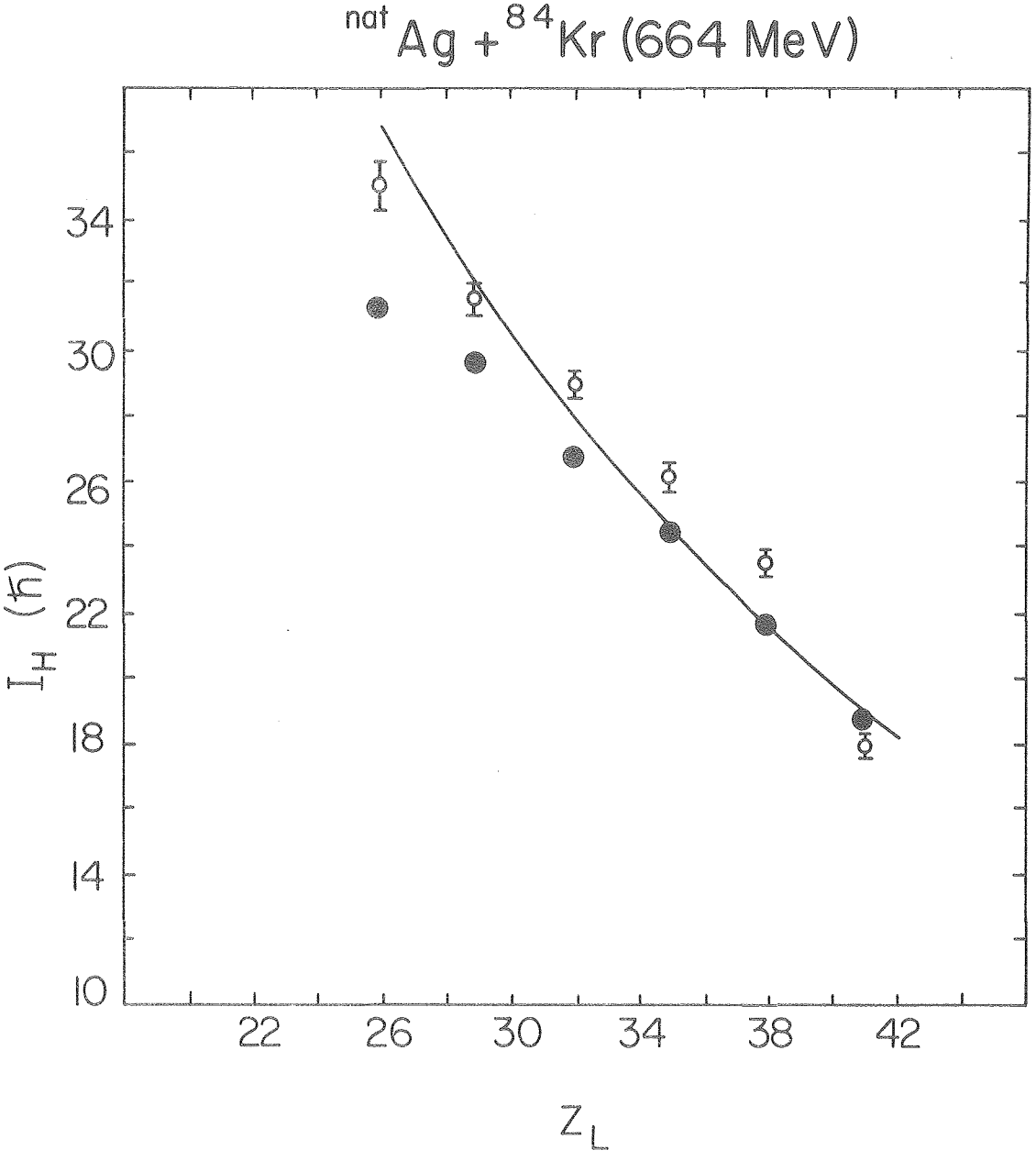

Fig. 7

XBL 8010-2228

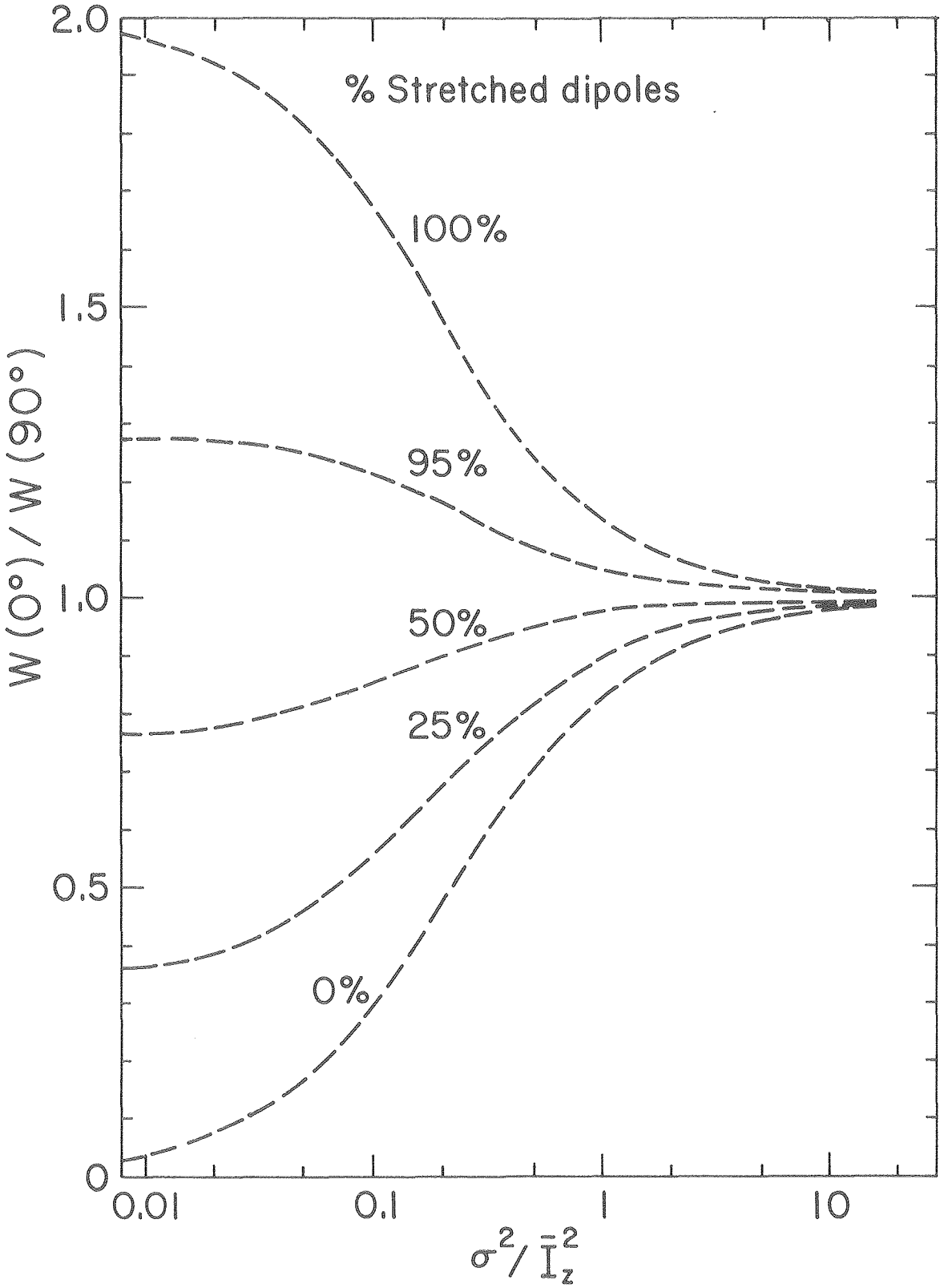

Fig. 8a

XBL 807-1673

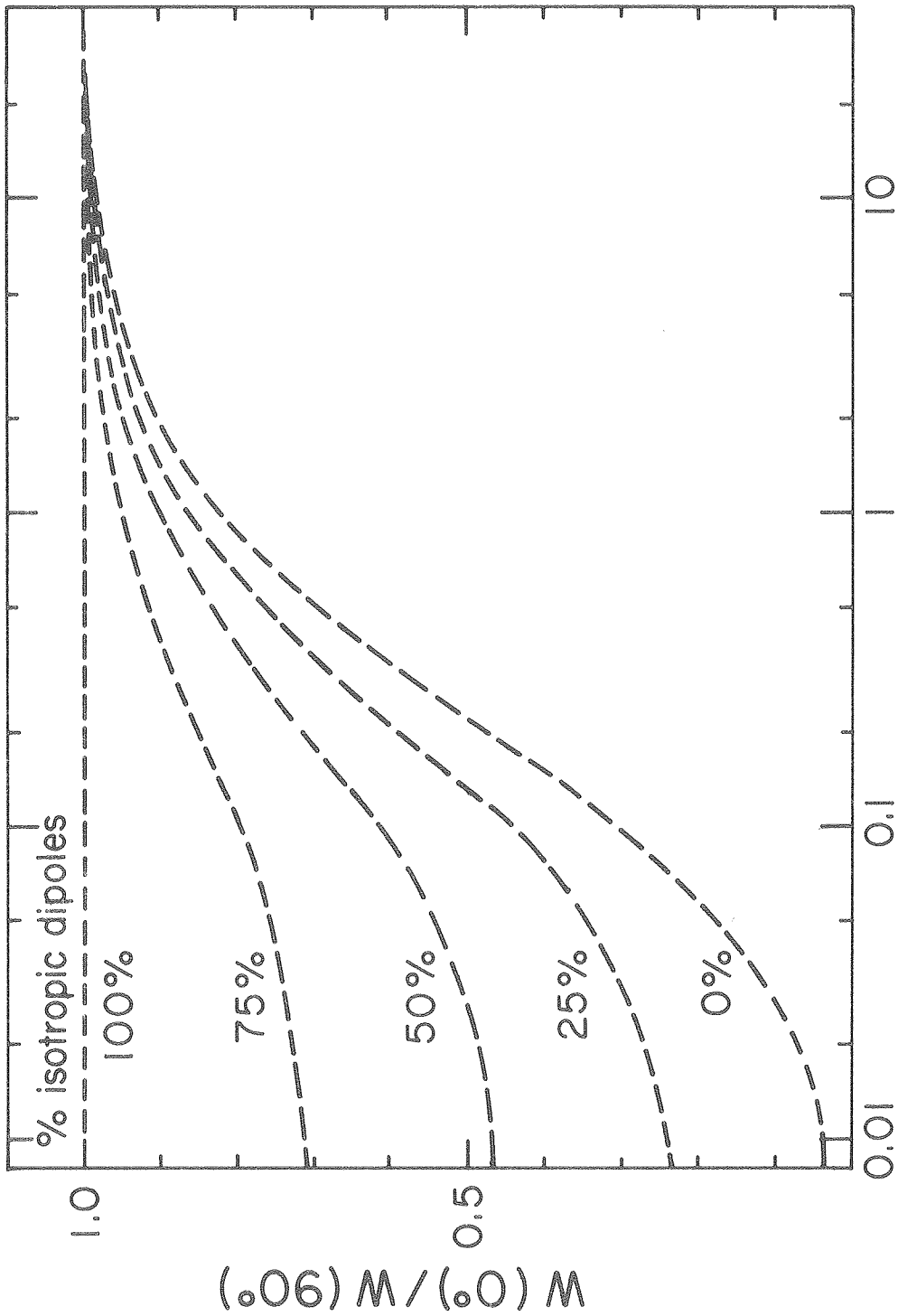

XBL 807-1671

Fig. 8b

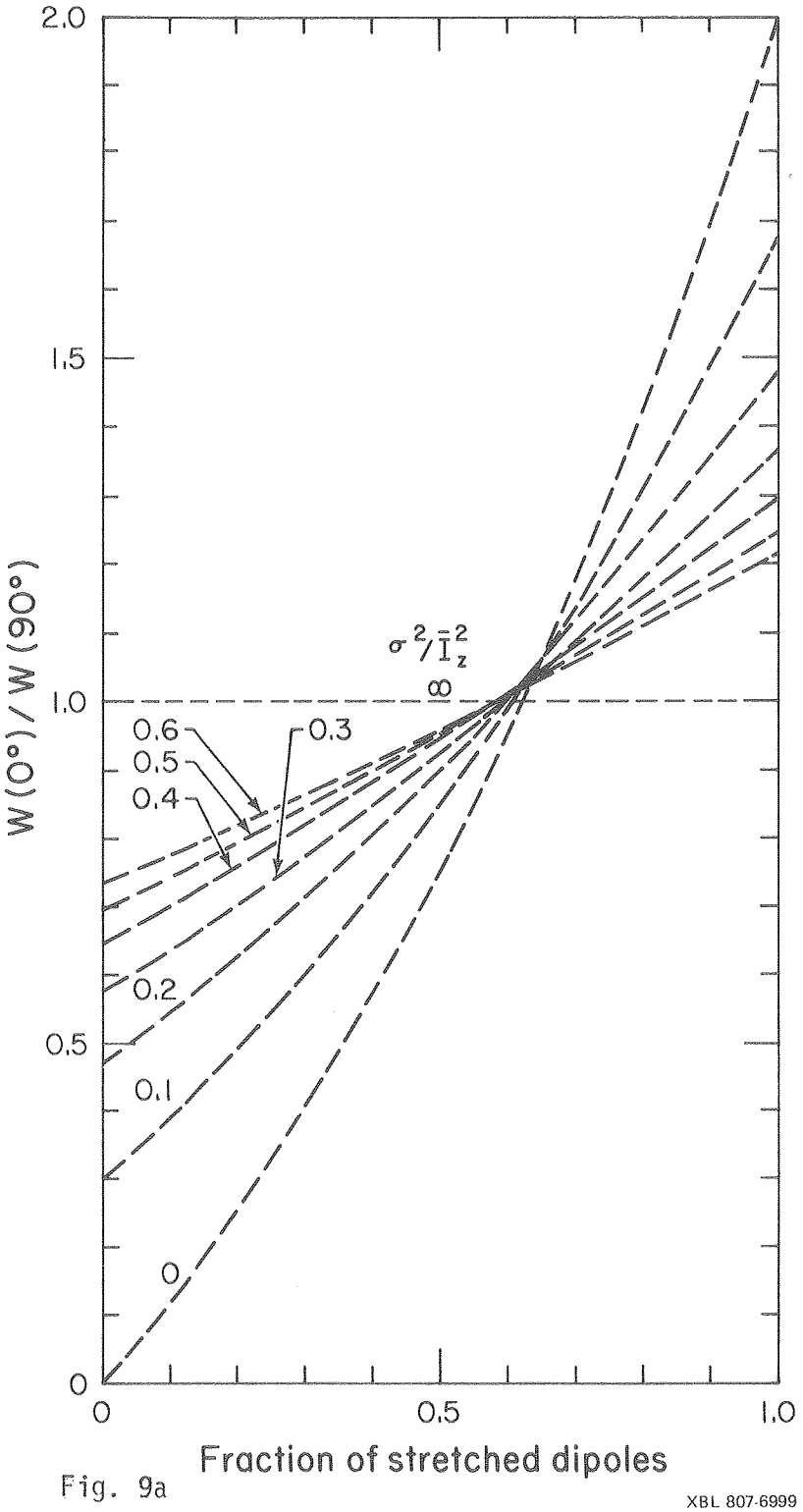

Fig. 9a

XBL 807-6999

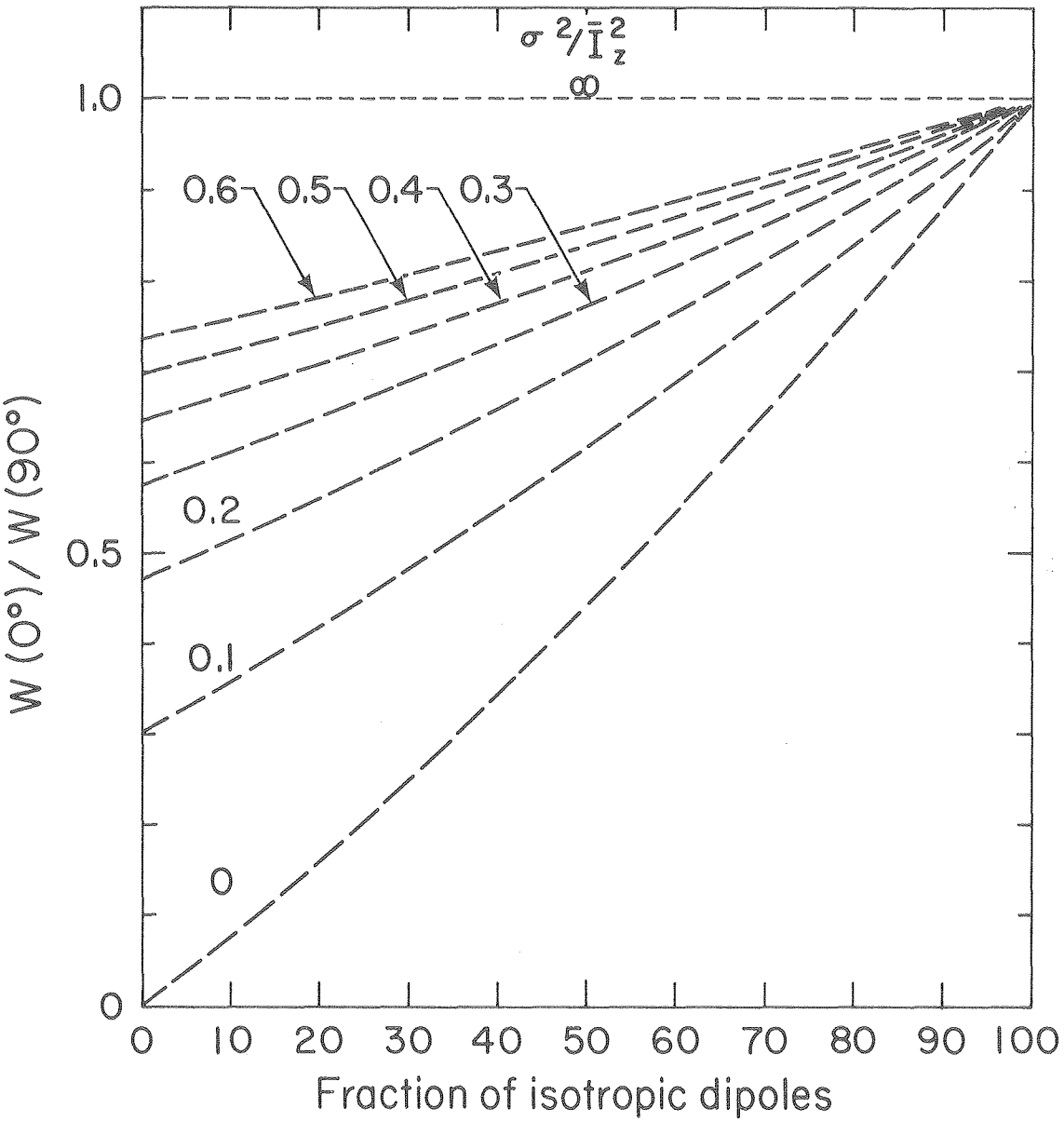

Fig. 9b

XBL 807-1670

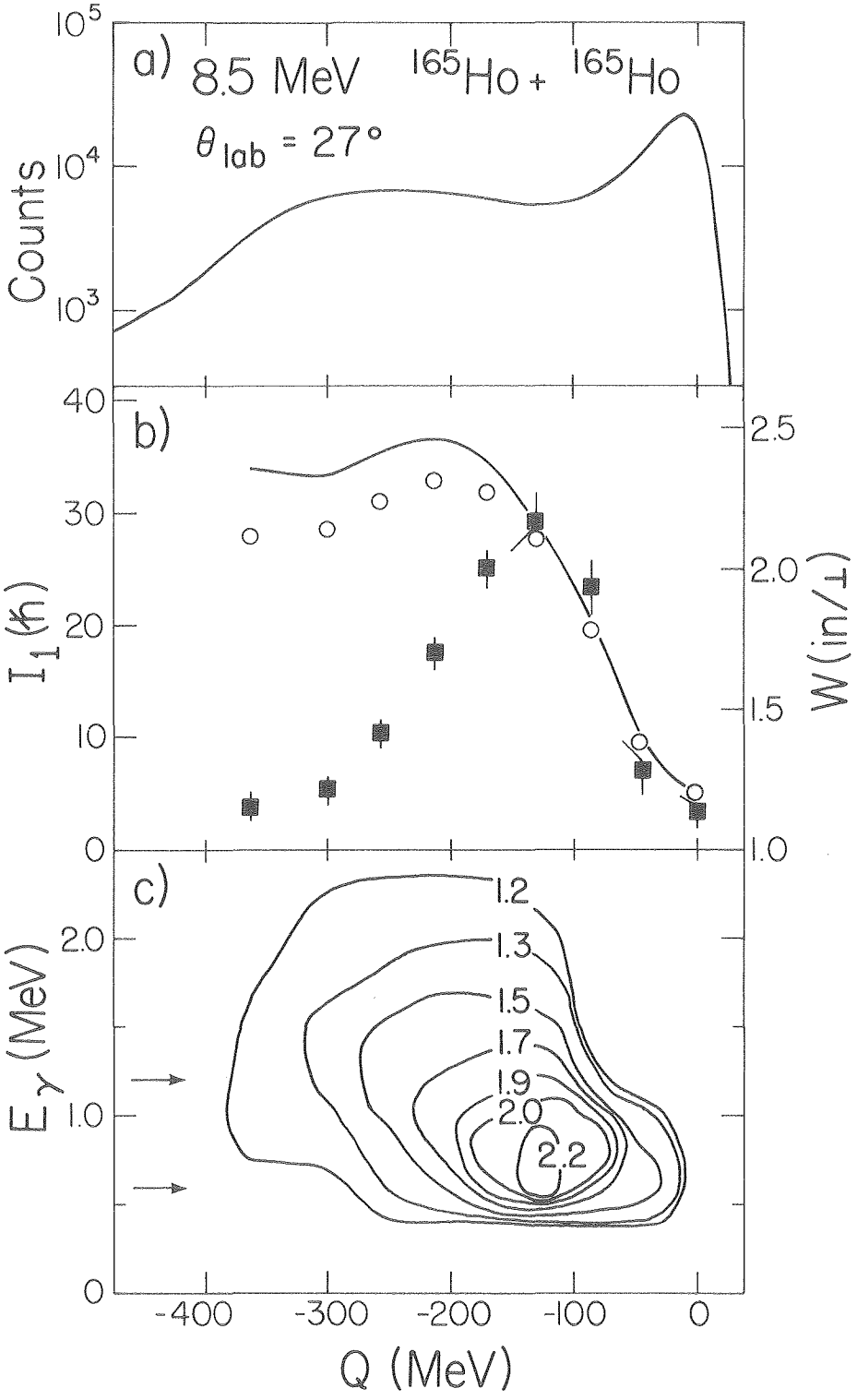

Fig. 10

XBL 806-1214

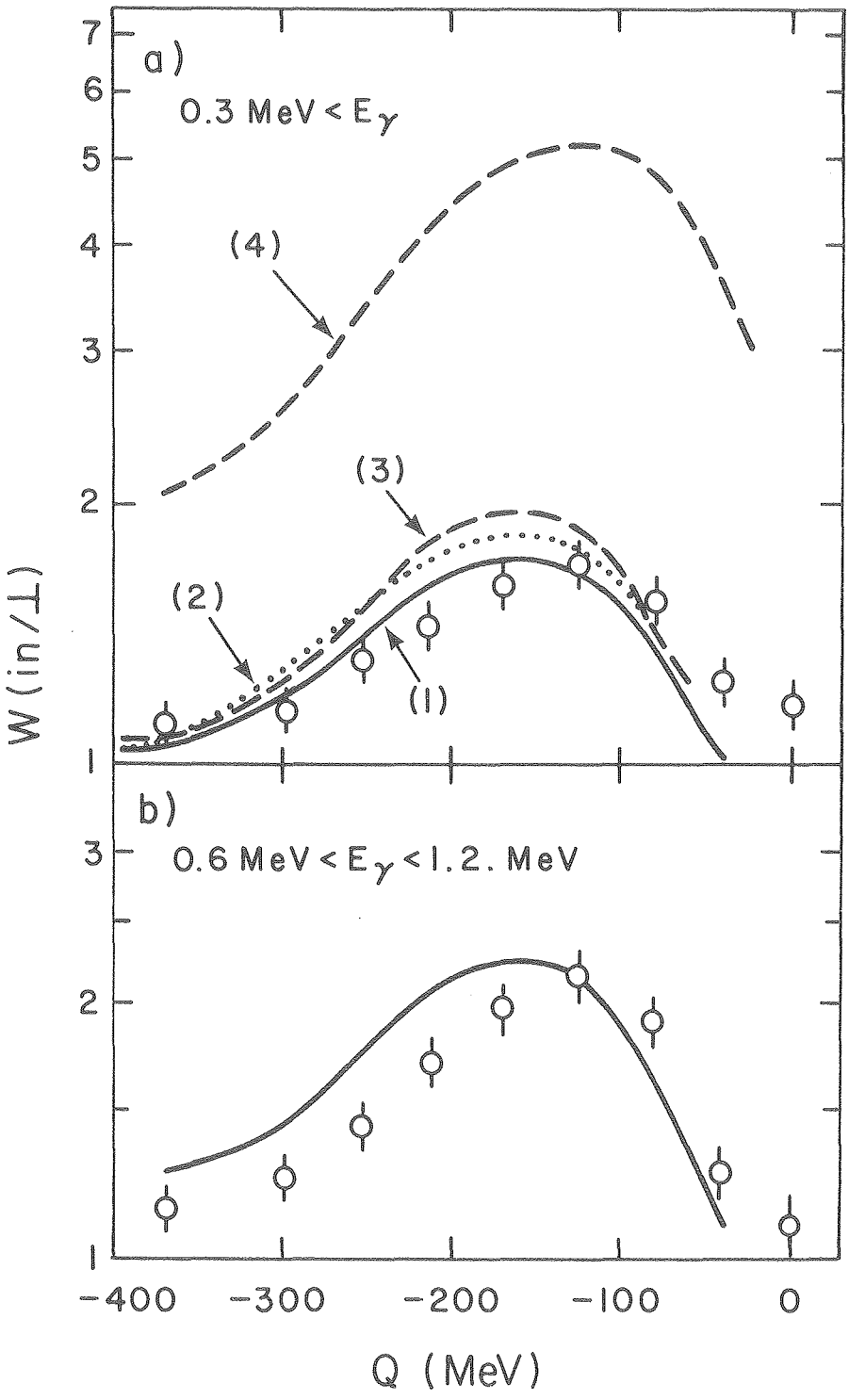

Fig. 11

XBL806-1193